Nanoclay Dispersion into a Thermosetting Binder Using Sonication and Intensive Mixing Methods

Havva Tutar Kahraman,[1,2] Halil Gevgilili,[1] Dilhan M. Kalyon,[1] Erol Pehlivan[2]

[1]Department of Chemical Engineering and Material Science, Stevens Institute of Technology, Hoboken, New Jersey 07030
[2]Department of Chemical Engineering, Selçuk University, Konya 42079, Turkey
Correspondence to: D. M. Kalyon (E-mail: dkalyon@stevens.edu)

ABSTRACT: Suspensions of epoxy with 10% by weight of organomodified montmorillonite clay [Cloisite 30B], prepared by two different methods, viz. intensive batch mixing and sonication, were investigated. The characterization of linear viscoelastic material functions of the suspension using small-amplitude oscillatory shear during processing enabled the assessments of the dispersion capabilities of the two mixing methods. Thermal imaging was used to monitor the temperature distributions generated during mixing. Sonication was determined to be more effective in the dispersion of the clay into the epoxy resin than the intensive batch mixing process, as revealed by the significant increase of the dynamic properties upon sonication, which suggested that some degree of intercalation and exfoliation had taken place during sonication. The use of the linear viscoelastic material functions thus provided a relatively easy to implement method for the analysis of the dispersion effectiveness of the different processing methods and operating conditions. © 2012 Wiley Periodicals, Inc. J. Appl. Polym. Sci. 129: 1773–1783, 2013

INTRODUCTION

Thermosetting polymers, including epoxy resins, are widely used especially in automotive, marine, coating, and aerospace industries.[1] The applications of thermosetting resins in general and epoxy resins in particular can be broadened further upon incorporation of various inorganic and organic reinforcements and fillers to especially improve the stiffness, toughness, and mold shrinkage of the resulting thermosetting composites, as well as possibly reduce costs.[2–6] Among the inorganic nanofillers, nanoclays offer potentially improved heat resistance, moduli and optical properties, decreased permeability, and flammability.[4,7–17] However, the incorporation of the nanoclay particles into the thermosetting matrix via solution processing, *in situ* polymerization and polymer melt processing, is a challenge.[4,18–27] Ideally, the concentration and the processing conditions should be selected so that the bulk of the clay tactoids are intercalated by the thermosetting polymer and the clay layers are separated from each other, i.e., exfoliated[18,20,28–30] as depicted in Figure 1.

There are conflicting reports in the literature regarding the comparative dispersion effectiveness of various methods, including sonication and intensive mixing,[2,31] for the compounding of nanoclays. For example, Dean et al.[32] reported conditions for exfoliation of clay particles in epoxy-nanoclay systems using sonication, whereas shear mixing did not achieve exfoliation. In contrast, Zunjarrao et al.[21] determined that more homogeneous epoxy/clay dispersions could be achieved by shear mixing (as attested by improved mechanical properties) in comparison with those processed by sonication. It is clear that a number of factors including the concentration of the clay, the operating conditions used, and the processing geometries would play roles in determining which dispersion method would be suitable for a given set of materials. However, such comparative studies are encumbered by the high cost of the typical structure analysis methods used in the assessment of the dispersion effectiveness, i.e., X-ray diffraction analysis (XRD) and transmission electron microscopy (TEM). Not only are such methods costly but they also require a large number of samples to be characterized. Furthermore, when the clay concentration is relatively high (e.g., at 10% by weight as encountered in this investigation), it will be difficult for the thermosetting polymer to intercalate and/or exfoliate the bulk of the clay tactoids. Thus, the dispersion process is principally expected to breakdown the particle sizes of the clay agglomerates, while still introducing limited intercalation and exfoliation. Under these circumstances, the use of the conventional tools for the assessment of intercalation and exfoliation, i.e., XRD and TEM, would be of limited use because the
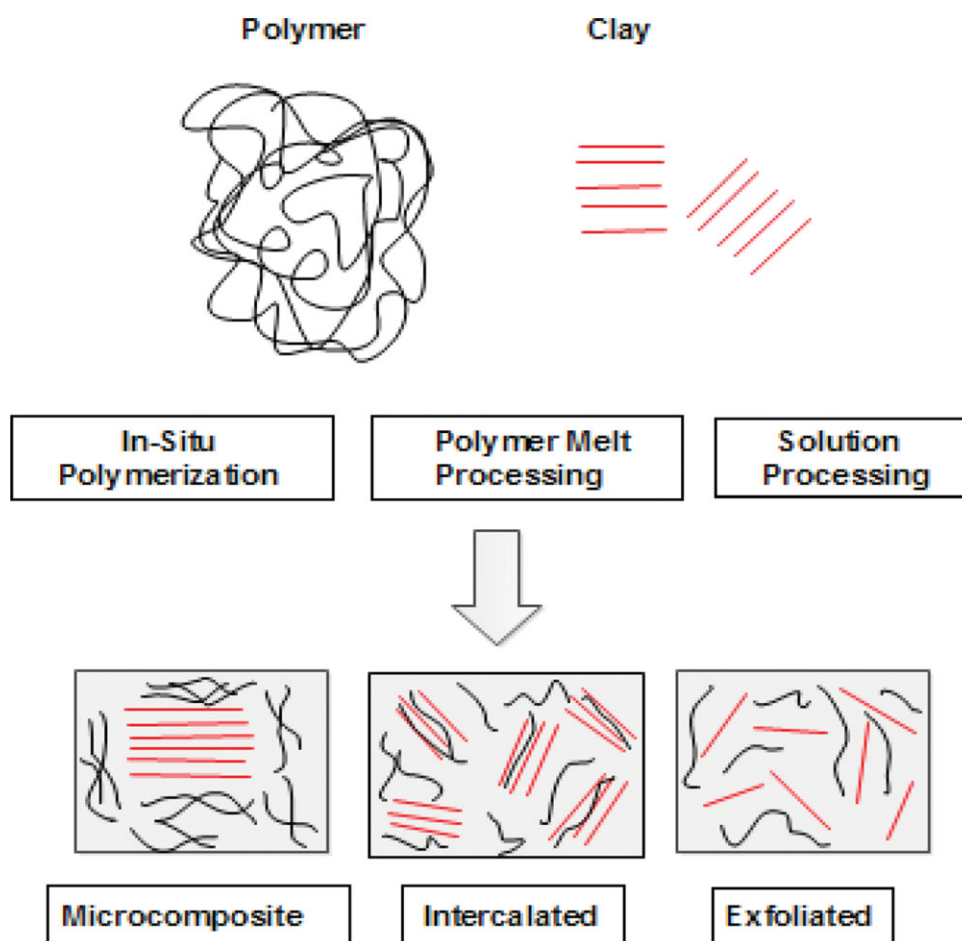
Figure 1. Schematic representation of preparation of polymer-clay nanocomposites. [Color figure can be viewed in the online issue, which is available at wileyonlinelibrary.com.]

bulk of the clay particles are expected to remain as tactoids. Rheological characterization methods are relatively easy to implement and can be used in the characterization of the dispersion effectiveness of various processing methods because the rheological material functions, especially the dynamic properties, are very sensitive to the microstructural distributions.[1,11–13] Here, the linear viscoelastic material functions of suspensions of clay in epoxy binder are characterized to assess and compare the dispersion effectiveness of sonication versus intensive batch mixing.

GENERAL BACKGROUND

Intensive Batch Mixing

Mixing tasks can be classified as extensive and intensive.[33] In extensive mixing, two or more starting components are interspersed in space with one another without changing the physical properties. On the other hand, intensive (dispersive) mixing describes multitude of processes in which intrinsic changes in the physical chacteristics of one or more components take place during processing.[33–35] During the preparation of clay suspensions, dispersive mixing, which breaks up the clay agglomerates and tactoids, can be achieved upon forcing the polymer/clay suspensions repeatedly into geometries with small gaps and relatively high-wall velocities. The agglomerates can rupture

when stress magnitudes (magnitude of the stress tensor), induced by viscous drag on the particles, exceed a certain threshold value, i.e., the cohesive force holding the agglomerate together.[33] For example, in the rubber industry, Banbury mixers and twin screw extruders are typically used as the batch and continuous means to impart relatively high stress magnitudes to enable the dispersion of carbon black and silica agglomerates. Here, a mini-Banbury mixer with relatively small gaps, and which is able to achieve high velocity differences between rotating and stationary surfaces, was used for the intensive mixing of the clay and epoxy suspensions.

Sonication

The sonication technology is a popular method for the generation of nanocomposites.[36,37] The main mechanism for the dispersion of particle tactoids and agglomerates by ultrasound technique is cavitation, i.e., the formation, growth, and sudden collapse of bubbles in suspensions. During such cavitation, high temperatures (as high 5000 K) are reached and pressures can be as high as 1000 atm.[38] A number of investigators have aimed to characterize the temperature development during sonication.[37,39,40] Chowdhury et al.[37] used a pulser cycle (turning on and off-time ratio) to control the temperature of the mixture during sonication to generate clay-epoxy nanocomposite by
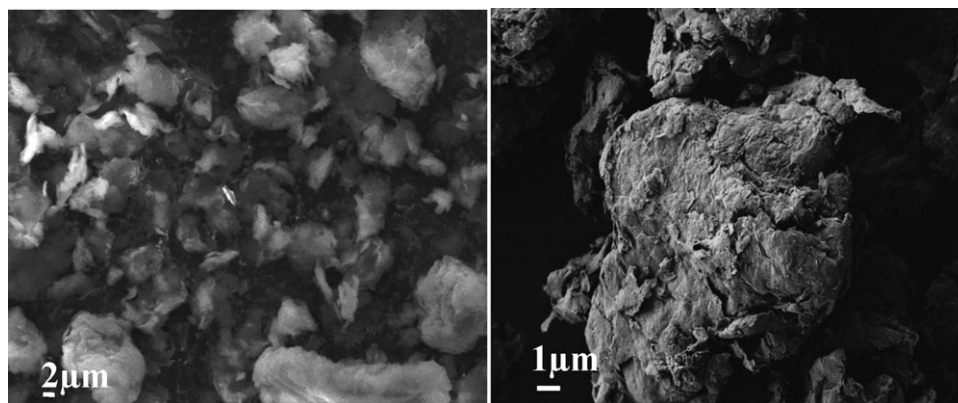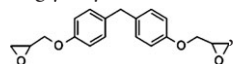
Figure 2. SEM micrographs of clay particles.

monitoring a single-point temperature via an infrared thermometer. Higaki et al.[39] measured the bulk temperature via a thermocouple and showed that the bulk temperature increased by 80°C soon after the sonication of tripalmitoylglycerol was initiated. Chu et al.[40] showed that the bulk temperature of the waste-activated sludge exceeded 50°C within 2 min during sonication. In our experiments, thermal imaging, which allows the characterization of the distribution of the temperature over a relatively large free surface surrounding the sonication horn, was used to monitor the temperature changes occurring during sonication more accurately. Thermal imaging was also used during intensive batch mixing.

EXPERIMENTAL

Materials
Diglycidyl ether of bisphenol F epoxy resin (DGEBF) , RAR-9283, which is a low-viscosity epoxy resin (density = 1.20 g cm^{-3} at 25°C) that reacts with a wide range of curing agents was procured from Royce International Corporation of East Rutherford, NJ. At 25°C, the magnitude of the complex viscosity of the epoxy was constant (frequency independent) at 3.5–4 Pa s, and the values of its loss moduli were approximately two orders of magnitude greater than the storage moduli indicating that the epoxy resin can be considered as a Newtonian fluid. The epoxy resin is recommended to be used with an aliphatic amine-based curing agent, RA-9837, available from Royce International Corporation of East Rutherford, NJ. However, in our dispersion experiments, the cross-linking agent was not included so that the changes in rheological material functions were only related to the state of the dispersion of the clay within the epoxy matrix and not to the possible premature curing of the thermosetting system. The only experiments which used the curing agent were for TEM based imaging experiments which required cross-linked samples. An organo-montmorillonite (MMT) clay (Cloisite 30B, Southern Clay Products, Gonzales, TX), modified with m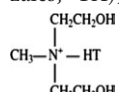ethyl, tallow, bis(2-hydroxyethyl) quaternary ammonium (MT2EtOH) ion, was used as the clay filler. The MMT clay is the most commonly used layered silicate for the preparation of polymer nanocomposites.

Figure 2 shows typical SEM micrographs of the organo-MMT clay particles. The typical sizes of the clay particles were in the range of 2–20 μm. The specific gravity was around 1.98.

Dispersion Experiments
Before both the intensive mixing and sonication experiments, the clay particles were dried for 24 h at 60°C under vacuum, and the epoxy resin was heated to 60°C. For both mixing methods, the clay particles were first gently blended into the epoxy resin at 60°C using a magnetic stirrer over 1.5 h. The mixture was subjected to sonication or intensive batch mixing for 0–30 min. The resulting suspensions were degassed under vacuum for 2 h. Upon degassing, the dynamic properties of the suspensions were characterized. For the preparation of the TEM and XRD samples, the curing agent was incorporated by being manually kneaded into the clay-epoxy suspension, and the mixture was cast into a rectangular mold cavity and allowed to cure at ambient temperature for 3 days before microtoming.

Sonication
A Misonix XL2020 ultrasonic processor was used at a frequency of 20 kHz and at ~18% of its maximum power output, i.e., at 108 W. The duration of the sonication was systematically changed up to 30 min. To achieve a fair comparison, all samples were sonicated in similar 50-mL jacketed containers. During sonication, the horn was placed at the same vertical position above the bottom of the container, and the fluid height was kept constant. Water at 21°C was circulated at the jacket of the container during sonication. Figure 3 shows the schematic representation of the sonication setup.

Intensive Batch Mixing
A mini-Banbury mixer, manufactured by Haake Buchler Instruments, Saddle Brooke, NJ (EU-5 V), with a mixing volume capacity of 60 mL, was used to mix the clay particles with the epoxy resin. The mixing chamber was operated at 70% full capacity, at 64 rpm, and at ambient temperature. The batch mixer was used with roller blade type agitators, which are typically used for high-intensive shearing applications for compounding of thermoplastic and thermosetting resins with rigid fillers.
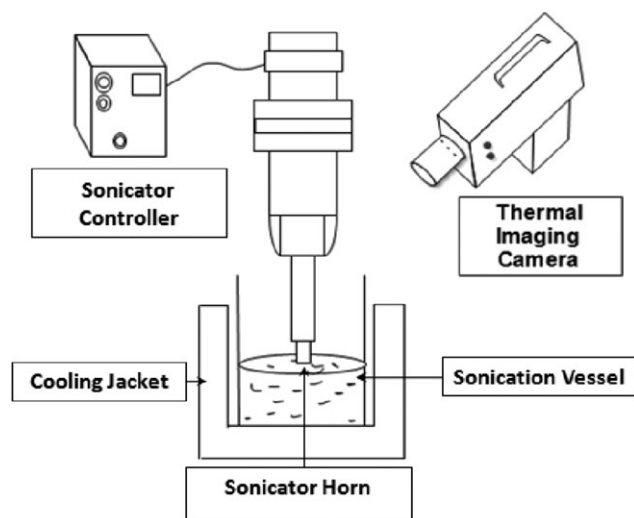
Figure 3. Schematic representation of the sonication setup.

Thermal Imaging

A thermal imaging camera (Inframetrics PM290) was used during both sonication and intensive batch mixing to monitor the temperature distributions generated during mixing.

Structural Characterization

The optical homogeneity of dispersions of epoxy resin and nanoclay was examined using a polarizing optical microscope (Nikon, Optiphot2-POL). Zeiss Auriga Small Dual-Beam FIB-SEM was also used. Cured TEM samples were microtomed using a Leica UCT microtome equipped with a diamond cutting knife. TEM samples were ∼70 nm thick and were analyzed using a Philips CM20 field-emission gun (FEG) scanning transmission electron microscope (TEM/STEM). Some of the cured samples were also subjected to XRD analysis using a Rigaku (Ultima IV) diffractometer.

Rheological Characterization

Rheological characterization involving small-amplitude oscillatory shear was carried-out using an Advanced Rheometric Expansion System rheometer available from TA Instruments of New Castle, DE in conjunction with 25 and 50-mm parallel plate fixtures. During oscillatory shearing, the specimen is sandwiched in between two disks, one of which is oscillating and the second one is stationary. The shear strain, γ, varies sinusoidally with time, t, at a frequency of ω, i.e., $\gamma = \gamma^0 \sin(\omega t)$. The shear strain amplitude $\gamma^0 = \theta D/h$, where θ is the angular displacement, D is the disk diameter, and h is the gap in between the two disks. The shear stress, τ, response to the imposed oscillatory deformation consists of two contributions associated with the energy stored as elastic energy and energy dissipated as heat, i.e., $\tau = G'(\omega) \gamma^0 \sin(\omega t) + G''(\omega) \gamma^0 \cos(\omega t)$. $G'(\omega)$ is the shear storage modulus which represents the energy stored as elastic energy, and $G''(\omega)$ is the shear loss modulus which represents viscous dissipation. In the region of linear viscoelasticity, the values of dynamic material properties, namely, the storage modulus, $G'(\omega)$, the loss modulus, $G''(\omega)$, the magnitude of complex viscosity, $\eta^\star(\omega) = [(G'/\omega)^2 + (G''/\omega)^2]^{1/2}$, and $\tan \delta = G''/G'$ are independent of the strain amplitude, γ^0.

To determine the strain amplitude range over which linear viscoelasticity prevails, strain sweep experiments were carried out in the strain amplitude range of 0.01–100%. The range of strain amplitudes over which linear behavior prevails (under which the dynamic data are independent of the strain amplitude) were found to be different for suspensions subjected to different dispersion conditions. The frequency dependent dynamic properties were characterized at the high ends of the strain amplitude ranges over which linear behavior prevails. The frequency range was 0.1–100 rps.

RESULTS AND DISCUSSION

Sonication Experiments

Figure 4 shows the typical temperature distributions observed at the free surfaces of epoxy/clay suspensions during sonication for 1, 10, and 20 min. After 20 min, the temperature distribution remained constant (results not shown). Figure 4 indicates that mixing of 10% by weight clay into the epoxy via sonication gives rise to a change of mean temperature of about 33°C, i.e., from 24 to 57°C. On the other hand, the values of the maximum temperature reach as high as 113°C. In the presence of the anionic and cationic sites on the Cloisite 30B clay platelets, the self-polymerization of the DGEBF epoxy binder commences around 300°C.[4]

The consequence of the observed hotspot formation is the necessity to prevent the crosslinking of the thermosetting system, while the sonication is on-going. In our experiments, this was accomplished by not mixing the cross-linking agent (curing agent) into the binder during the compounding of the clays into the epoxy binder. If the cross-linking agent were to be also included in the formulation during the mixing of the clay particles into the binder phase, there would have been some premature crosslinking. Because we are relying on the monitoring of the dynamic properties for the assessment of the dispersion, changes in the dynamic properties due to premature curing would have complicated the interpretation of our findings, as well as rendering the dispersion of the clay particles into the epoxy more difficult.

The characterization of the dynamic properties over a wide range of frequencies allows the fingerprinting of the structure and the resulting viscoelastic response over a broad characteristic time scale. In general, at relatively small characteristic times for deformation (relatively high frequencies), the elastic response is accentuated, whereas at longer characteristic times (relatively low frequencies) the viscous response dominates. The effects of the sonication duration on the development of the dynamic properties are shown in Figures 5–8, where the frequency dependencies of the storage modulus, $G'(\omega)$, loss modulus, $G''(\omega)$, magnitude of complex viscosity, $\eta^\star(\omega)$, and loss tangent, $\tan \delta(\omega)$, are provided. In these figures, the ranges pertain to the 95% confidence intervals determined according to Student's t distribution.

Mixing of the clay into the epoxy resin via sonication for only 10 min increases the storage modulus values, $G'(\omega)$ (indicative of the energy stored as elastic energy), by about an order of magnitude in comparison with the storage moduli of the epoxy/clay
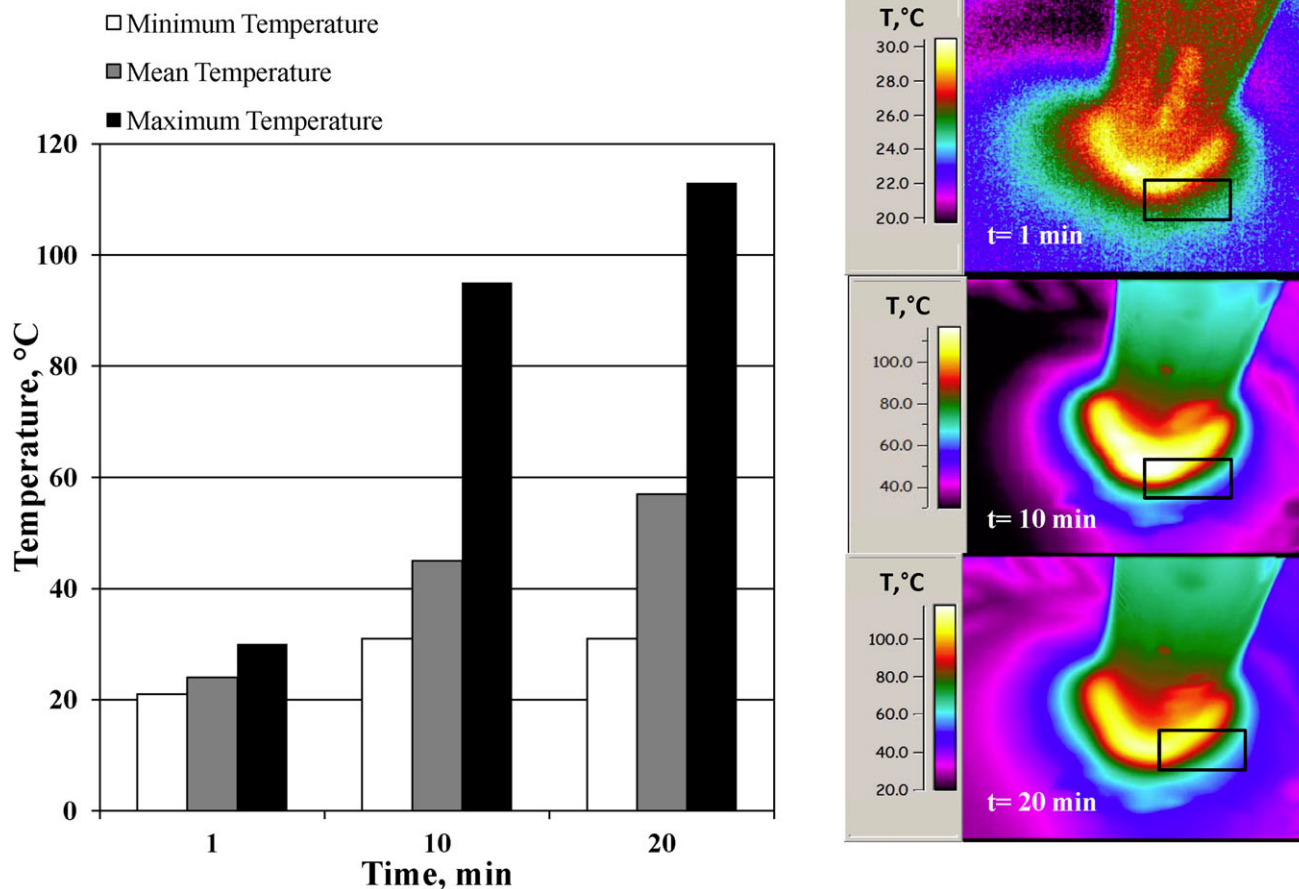
Figure 4. Temperature distributions at the free surfaces of epoxy/clay suspensions during sonication. [Color figure can be viewed in the online issue, which is available at wileyonlinelibrary.com.]
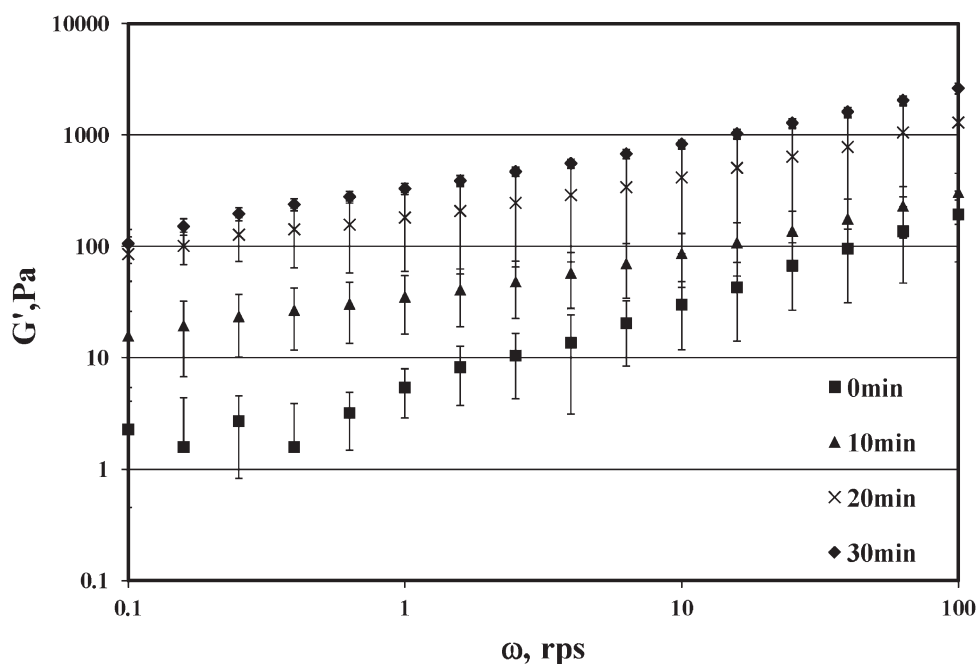

Figure 5. Storage modulus, G', versus frequency, ω, of epoxy suspension with 10% clay at different sonication durations of 0, 10, 20, and 30 min.
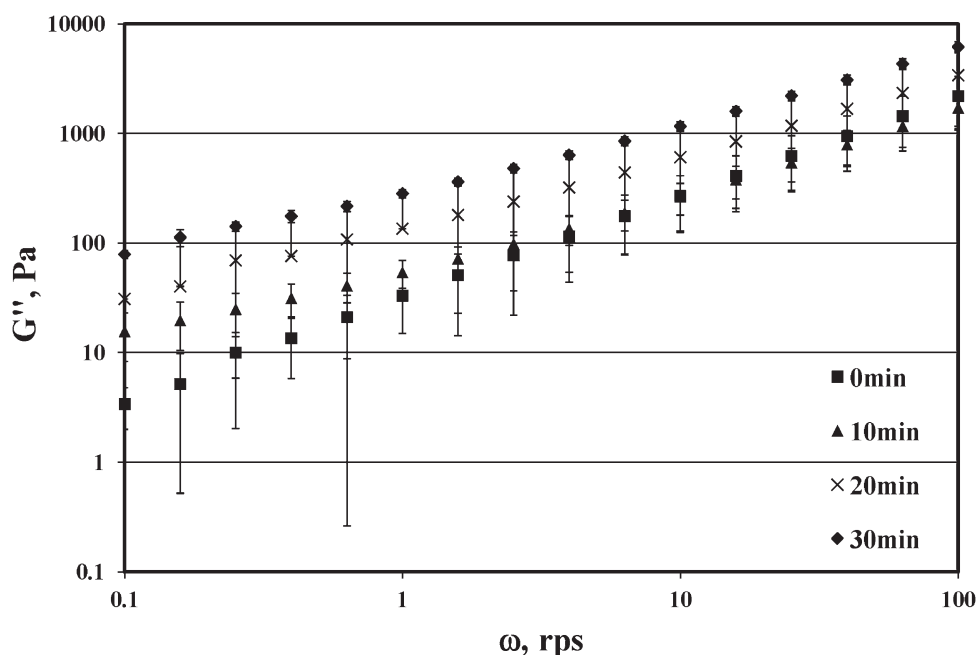
Figure 6. Loss modulus, G'', versus frequency, ω, of epoxy suspension with 10% clay at different sonication durations of 0, 10, 20, and 30 min.

system gently stirred before sonication. The presence of the alkylammonium ions on the clay platelet surfaces allows the epoxy resin to wet and penetrate into the gallery space between the platelets as well as to increase the elasticity and the viscosity of the suspension. With the increase of the sonication duration from 10 to 20 min greater penetration of the epoxy into the gallery spaces, increases the storage modulus values further (e.g., the mean values determined at 0.1 rps increase from 15.8 to 85.5 Pa). The rate of increase of the storage modulus values with sonication duration decreases with increasing sonication time. In the presence of the curing agent, the polymerization of the epoxy would have taken place within the gallery spaces, possibly leading to the separation and exfoliation of the nanoclay platelets.[4]

The loss modulus values, which are indicative of the energy dissipated as heat during one cycle of deformation and the magnitude of complex viscosity, η^*, values, also increase upon sonication duration (Figures 6 and 7). For example, the mean values of the loss modulus values at 0.1 rps increased from 3.4 to 79.0 Pa upon sonication for 30 min. On the other hand, the mean values of the magnitude of complex viscosity, η^*, increased from 40.8 to 1333.8 Pa s at $\omega = 0.1$ rps and from 17.4 to 67 Pa s at $\omega = 100$ rps. Generally, the dynamic properties are more sensitive to structure development at their low-frequency range. The tan δ values decrease with the increase of the sonication duration (Figure 8) indicating that the suspensions are achieving disproportionately great elasticity in comparison with viscous dissipation.

Overall, these dynamic properties reflect the changes in the structure of the clay particles occurring upon sonication. With increasing duration of sonication, the particle sizes of the clay agglomerates decrease and some of the gallery spaces of the clay tactoids are penetrated, i.e., intercalated, by the epoxy binder. During dispersion, some of the clay layers separate completely,

i.e., exfoliate. As earlier investigations have indicated at relatively high clay concentrations, the transformations associated with intercalation and exfoliation are never complete and the polymer/clay mixture is always a composite structure consisting of clay tactoids, intercalated clay, and exfoliated clay platelets.[24,27,29,30]

The typical TEM micrographs of a 30 min sonicated cured sample are shown in Figure 9. The clay tactoid particles originally exhibited particle sizes which were in the range of 2–20 μm. Upon dispersion via sonication intercalated structures, which are disordered and scattered within the polymeric binder phase and which exhibit little exfoliation, are generated. This is consistent with earlier studies.[4] The intercalation effect was accompanied with a decrease of the particle size of the clay tactoids.
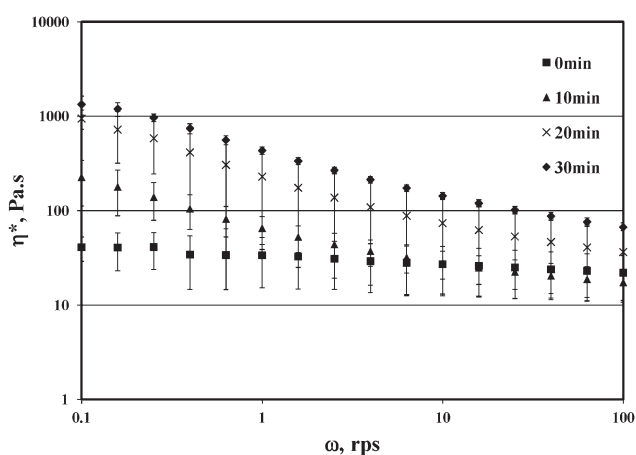

Figure 7. Magnitude of complex viscosity, η^*, versus frequency, ω, of epoxy suspension with 10% clay at different sonication durations of 0, 10, 20, and 30 min.
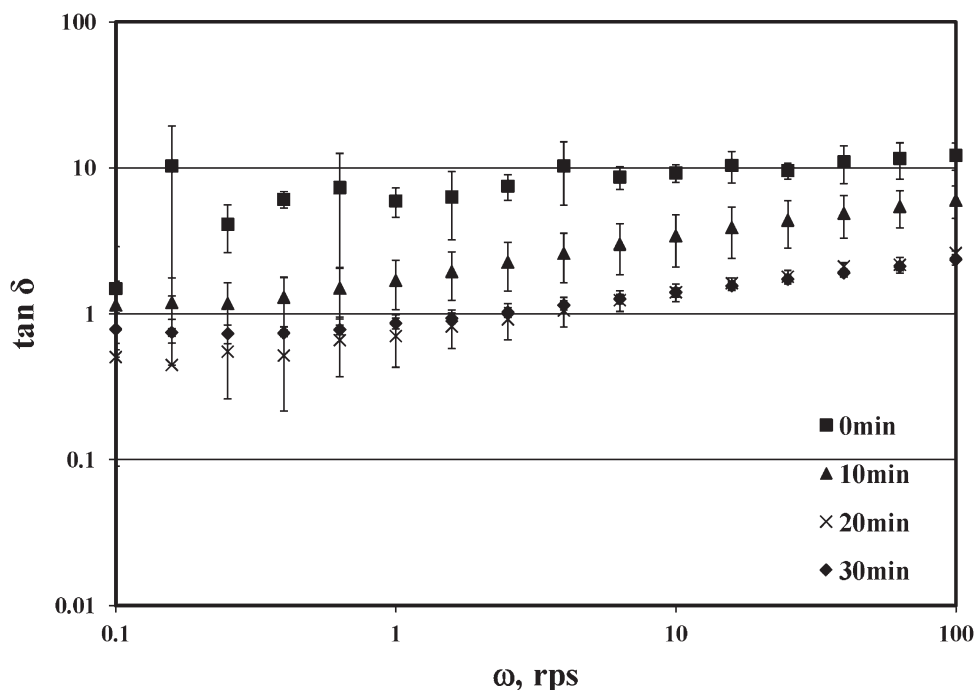
Figure 8. Tan δ, versus frequency, ω, of epoxy suspension with 10% clay at different sonication durations of 0, 10, 20, and 30 min.

The XRD results (not shown) indicated that the intercalation of the clay by the epoxy binder was masked by the presence of the clay tactoids which have persisted due to the relatively high concentration of clay (10% by weight) that is used. Nevertheless, even the limited intercalation and exfoliation observed in Figure 9 and the associated increase of the surface to volume ratio of the clay particles appear to be sufficient for the elasticity and the shear viscosity of the suspension to increase
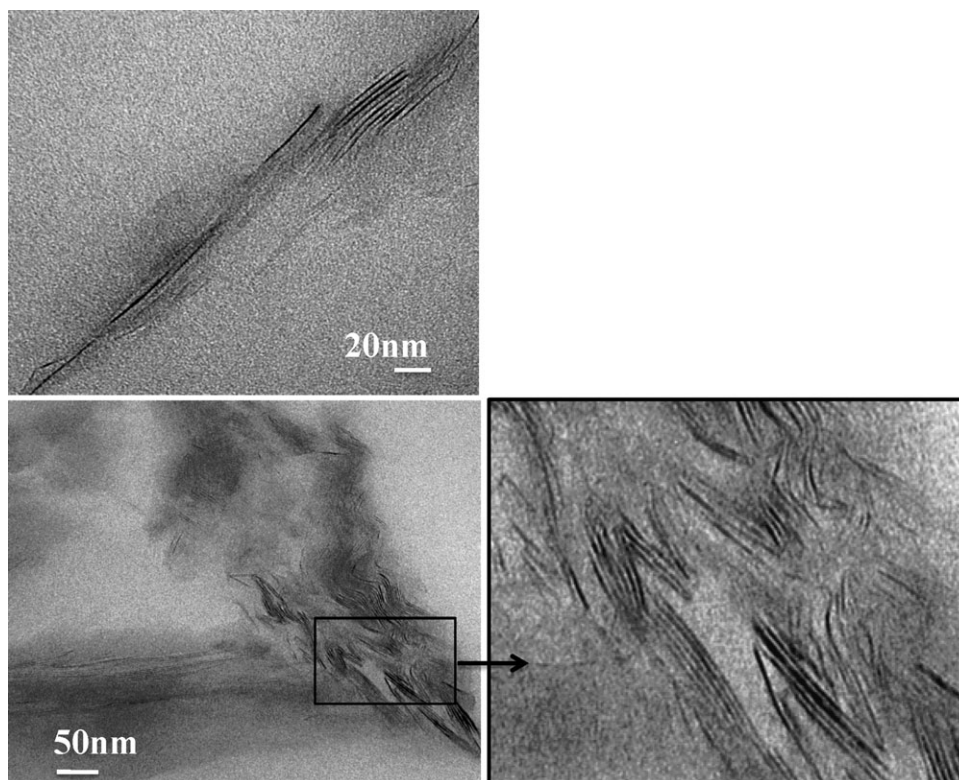

Figure 9. TEM micrographs of epoxy/clay suspension upon 30 min of sonication.
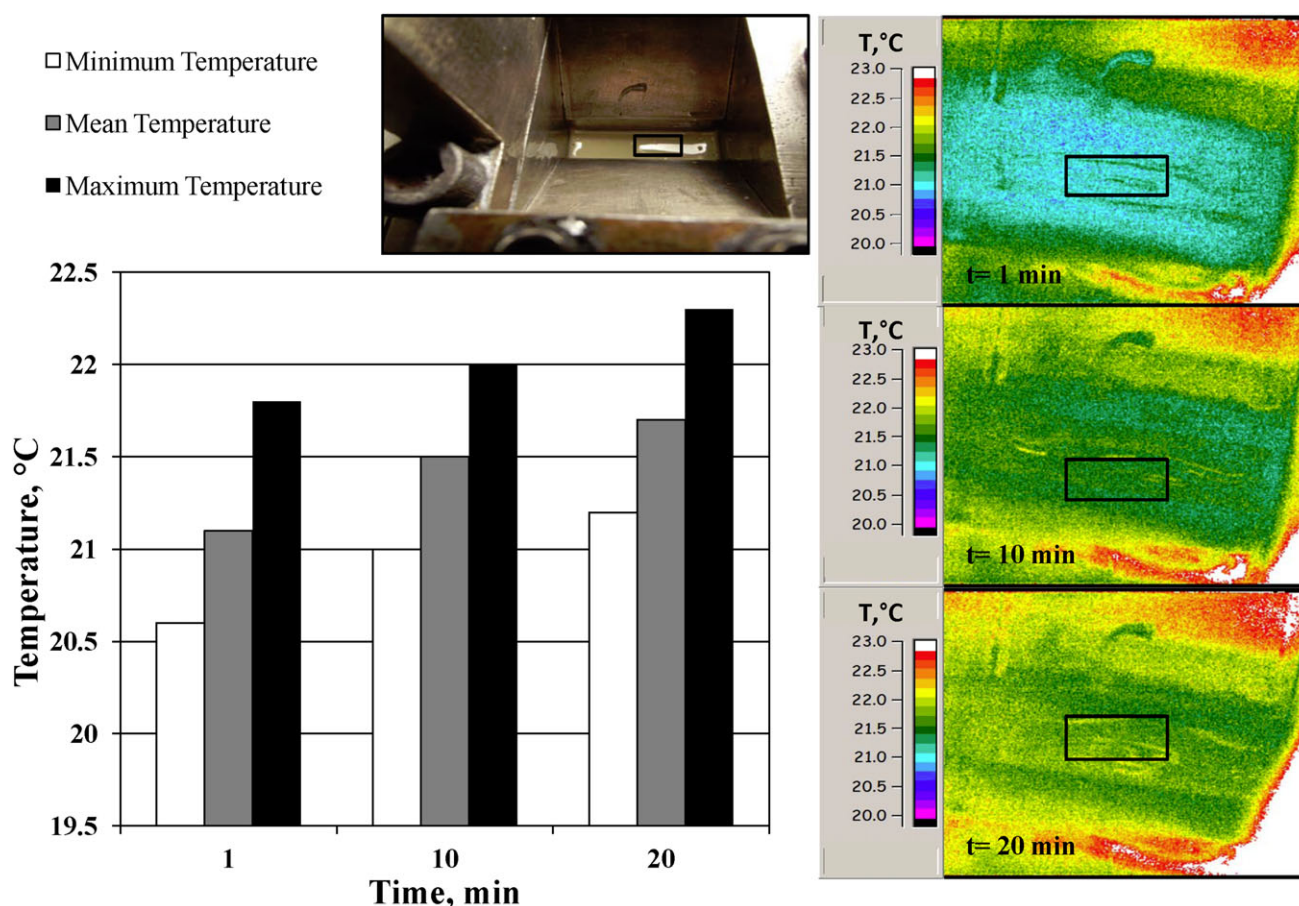
Figure 10. Temperature distributions at the free surfaces of epoxy/clay suspensions during intensive batch mixing process. [Color figure can be viewed in the online issue, which is available at wileyonlinelibrary.com.]

significantly. At smaller concentrations of the clay particles, greater extents of intercalation and exfoliation should take place.

It should be noted that for conventional mixtures of noncolloidal particles incorporated into a polymer melt the process of structuring and the resulting changes in the rheological behavior in the total absence of intercalation and exfoliation are very different. Kalyon et al. have shown that for noncolloidal graphite particles, which were initially agglomerated, the increase of the mixing time and the associated increase of the specific energy input progressively lead to the breakdown of the particle agglomerates and the encapsulation of the particles by the binder.[41–43] Initially, there is void space between the ultimate particles of the agglomerates. This void space contributes to the volume fraction of the solid phase. As the agglomerates are broken down during the dispersion process, the void space in between the ultimate particles becomes occupied by the binder and the yield stress and the shear viscosity, as well as the elasticity of the suspension, decrease.[41,42] This mechanism of breakdown of the particle agglomerates is expected to generate decreases in dynamic properties, which were indeed observed for non-colloidal graphite particles.[41–43] However, as indicated in Figures 5–8, in the case of nanosuspensions, dispersion of the nanoparticles results in orders of magnitude increase in vis-

cosity as well as elasticity, consistent with earlier investigations as a result of the significant increase of the surface to volume ratio of the particles upon intercalation and exfoliation.[44–46]

Intensive Batch Mixing

Unlike what is observed for sonication, the temperature rise during intensive mixing at ambient temperature was not significant, i.e., within $\pm 3^{\circ}C$ of the ambient temperature (Figure 10). This small temperature rise is indicative of the relatively low-viscous energy dissipation that could be imparted during intensive batch mixing. Because the viscous energy dissipation is represented by the product of the stress and velocity gradient tensors, a relatively low value is indicative of the limited deformation of the epoxy/clay suspension during intensive batch mixing.

The typical small-amplitude oscillatory shear behavior of epoxy/clay suspension samples prepared via intensive batch mixing are compared with those prepared via sonication in Figures 11 and 12. The dynamic properties, i.e., the magnitude of complex viscosity, η^*, and the storage modulus, G', values of the batch mixed samples have not increased appreciably during the 30 min of mixing in the intensive mixer. On the other hand, the dynamic properties η^* and G' of epoxy/clay suspensions, prepared using sonication, are significantly, i.e., orders of
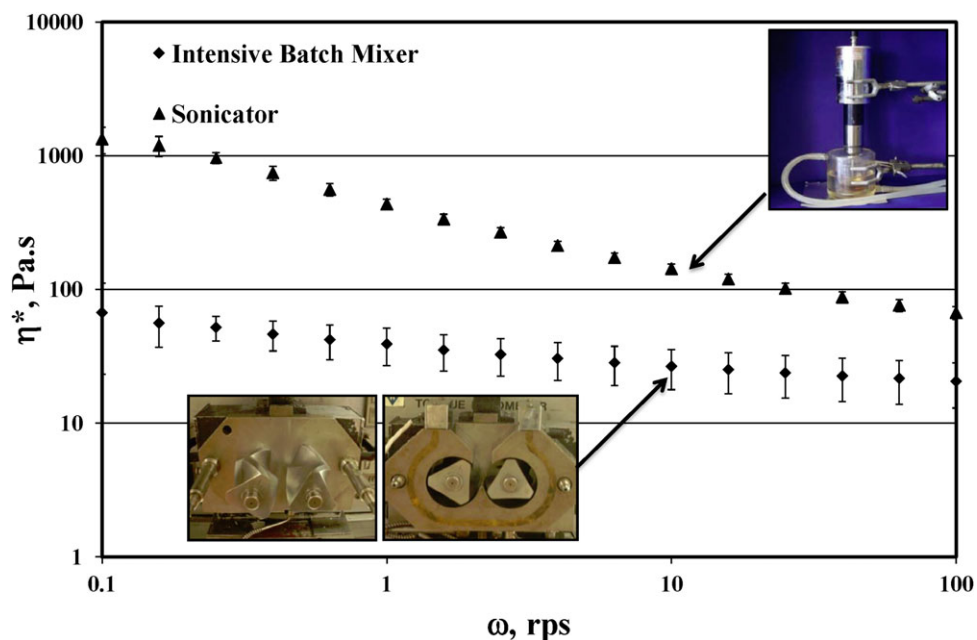
Figure 11. Comparison of the magnitude of complex viscosity, η^*, versus frequency, ω, behavior of epoxy suspension with 10% clay upon batch mixing and sonication. [Color figure can be viewed in the online issue, which is available at wileyonlinelibrary.com.]

magnitude, greater than those of the epoxy/clay suspensions prepared using intensive batch mixing (Figures 11 and 12). The rheological characterization results thus suggest that at least for the clay concentration used (10% by weight) the intensive batch mixing of the clay particles into the epoxy resin is not as efficient as the sonication process. Direct evidence of the dispersion

characteristics of the batch mixed and sonicated samples can be seen in the light microscopy images shown in the insets of Figure 12 which suggest that clay agglomerates are indeed significantly greater in size for the batch mixed samples in comparison to the epoxy/clay samples that are prepared by sonication. Sonication also gives rise to a significant increase of the
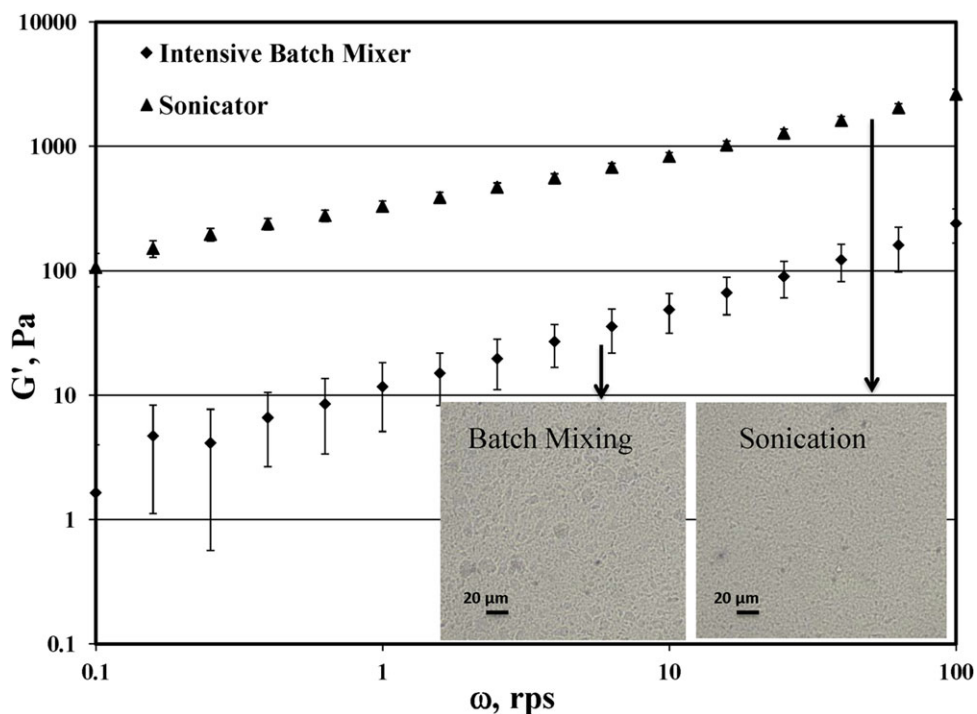

Figure 12. Storage modulus, G', versus frequency, ω, behavior of epoxy suspension with 10% clay upon intensive batch mixing and sonication and their typical light microscopy images.

amounts of intercalated and exfoliated clay platelets, which in turn leads to a greater extent of the immobilization of the epoxy binder that is in contact with the particles. Thus, greater increases in the dynamic properties are observed upon sonication in comparison with compounding via intensive batch mixing.

CONCLUSIONS

The preparation of epoxy/clay suspension system was investigated using intensive batch mixing and sonication. Dynamic properties were used to assess the dispersion effectiveness. Upon intercalation/exfoliation of the clay tactoids significant increase of the surface/volume ratio of the clay platelets occurs. This leads to the increase of the amount of immobilized epoxy resin that is in contact with the platelets and, hence, gives rise to significant increases in the viscosity and the elasticity of the resulting suspensions. On the basis of the comparisons of the dynamic properties monitored at the effectiveness end of the mixing processes, the sonication process is determined to be more effective in the dispersion of the clay particles and generation of nanoclays, in comparison with intensive mixing process for this epoxy/nanoclay system.

However, the better dispersion ability of the sonication process also leads to generation of temperature hot spots which can lead to premature curing of thermosetting resins. The consequence of this finding for the epoxy/clay system of this investigation is the removal of the curing agent from the mixture when the clay particles were being compounded, thus, suggesting the use of a two-stage process—first, dispersion of the clays into epoxy binder and intercalation/exfoliation, and then followed by the mixing of the curing agent into the epoxy-clay suspensions.

ACKNOWLEDGMENTS

REFERENCES

1. Oh, T.-K.; Hassan, M.; Beatty, C.; El-Shall, H. *J. Appl. Polym. Sci.* **2006**, *100*, 3465.

2. Singh, R. P.; Khait, M.; Zunjarrao, S. C.; Korach, C. S.; Pandey, G. *J. Nanomater.* **2010**, 352746.

3. Ingram, S. E.; Liggat, J. J.; Pethrick, R. A. *Polym. Int.* **2007**, *56*, 1029.

4. Ingram, S. E.; Pethrick, R. A.; Liggat, J. *J. Polym. Int.* **2008**, *57*, 1206.

5. McIntyre, S.; Kaltzakorta, I.; Liggat, J. J.; Pethrick, R. A.; Rhoney, I. *Ind. Eng. Chem. Res.* **2005**, *44*, 8573.

6. Lakshmi, M. S.; Narmadha, B.; Reddy, B. S. R. *Polym. Degrad. Stab.* **2008**, *93*, 201.

7. Isik, I.; Yilmazer, U.; Bayram, G. *Polymer* **2003**, *44*, 6371.

8. Tsai, T.-Y.; Wu, Y.-J.; Hsu, F.-J. *J. Phys. Chem. Solids* **2008**, *69*, 1379.

9. Mohan, T. P.; Kumar, M. R.; Velmurugan, R. *Polym. Int.* **2005**, *54*, 1653.

10. Zammarano, M.; Franceschi, M.; Bellayer, S.; Gilman, J. W.; Meriani, S. *Polymer* **2005**, *46*, 9314.

11. Demirkol, E.; Kalyon, D. M. *J. Appl. Polym. Sci.* **2007**, *104*, 1391.

12. Nassar, N.; Utracki, L. A.; Kamal, M. R. *Int. Polym. Process.* **2005**, *4*, 423.

13. Ghasemi, H.; Carreau, P. J.; Kamal, M. R.; Tabatabaei, S. H. *Polym. Eng. Sci.* **2012**, *52*, 420.

14. Cui, L.; Bara, J. E.; Brun, Y.; Yoo, Y.; Yoon, P. J.; Paul, D. R. *Polymer* **2009**, *50*, 2492.

15. Seyidoglu, T.; Yilmazer, U. *J. Appl. Polym. Sci.,* **2012**, *124*, 2430.

16. Yasmin, A.; Daniel, I. M. *Polymer* **2004**, *45*, 8211.

17. Yasmin, A.; Luo, J. J.; Abot, J. L.; Daniel, I. M. *Compos. Sci. Technol.* **2006**, *66*, 2415.

18. Park, J. H.; Jana, S. C. *Macromolecules* **2003**, *36*, 2758.

19. Timmerman, J. F.; Hayes, B. S.; Seferis, J. C. *Compos. Sci. Technol.* **2002**, *62*, 1249.

20. Luo, J.-J.; Daniel, I. M. *Compos. Sci. Technol.* **2003**, *63*, 1607.

21. Zunjarrao, S. C.; Sriraman, R.; Singh, R. P. *J. Mater. Sci.* **2006**, *41*, 2219.

22. Ceccia, S.; Turcato, E. A.; Maffettone, P. L.; Bongiovanni, R. *Prog. Org. Coat.* **2008**, *63*, 110.

23. Kornmann, X.; Lindberg, H.; Berglund, L. A. *Polymer* **2001**, *42*, 4493.

24. Basara, C.; Yilmazer, U.; Bayram, G. *J. Appl. Polym. Sci.* **2005**, *98*, 1081.

25. Decker, C.; Keller, L.; Zahouily, K.; Benharfi, S. *Polymer* **2005**, *46*, 6640.

26. Iqbal, K.; Khan, S.-U.; Munir, A.; Kim, J.-K. *Compos. Sci. Technol.* **2009**, *69*, 1949.

27. Hussain, F.; Chen, J.; Hojjati, M. *Mater. Sci. Eng. A* **2007**, *445–446*, 467.

28. Sancaktar, E.; Kuznicki, J. *Int. J. Adhes. Adhes.* **2011**, *31*, 286.

29. Landry, V.; Riedl, B.; Blanchet, P. *Prog. Org. Coat.* **2008**, *62*, 400.

30. Mittal, V. *Materials* **2009**, *2*, 992.

31. Gintert, M. J.; Jana, S. C.; Miller, S. G. *Polymer* **2007**, *48*, 4166.

32. Dean, K.; Krstina, J.; Tian, W.; Varley, R. *J. Macromol. Mater. Eng.* **2007**, *292*, 415.

33. Tadmor, Z.; Gogos, C. G. Principles of Polymer Processing; Wiley-Interscience, Hoboken, New Jersey, **2006**; p 196.

34. Middleman, S. Fundamentals of Polymer Processing; McGraw-Hill, New York, **1977**; p 295.

35. Kalyon, D. M. In Handbook of Polymer Science and Technology; Cheremisinoff, N. P., Ed.; Marcel Dekker, New York, **1989**; Vol. *3*, p 373.

36. Ma, P.-C.; Siddiqui, N. A.; Marom, G.; Kim, J.-K. *Compos. A* **2010**, *4*, 1345.

37. Chowdhury, F. H.; Hosur, M. V.; Jeelani, S. *Mater. Sci. Eng. A* **2006**, *421*, 298.

38. Mason, T. J.; Lorimer, J. P. Applied Sonochemistry; Wiley-VCH, **2002**; p 36.

39. Higaki, K.; Ueno, S.; Koyano, T.; Kiyotaka Sato, K. *J. Am. Oil Chem. Soc.* **2001**, *78*, 513.

40. Chu, C. P.; Chang, B.-V.; Liao, G. S.; Jean, D. S.; Lee, D. J. *Water Res.* **2001**, *35*, 1038.

41. Kalyon, D.; Dalwadi, D.; Erol, M.; Birinci, E.; Tsenoglu, C. *Rheol. Acta* **2006**, *45*, 641.

42. Erol, M.; Kalyon, D. *Int. Polym. Proc.* **2005**, *20*, 228.

43. Kalyon, D.; Birinci, E.; Yazici, R.; Karuv, B.; Walsh, S. *Polym. Eng. Sci.* **2002**, *42*, 1609.

44. Vural, S.; Dikovics, K.; Kalyon, D. *Soft Matter* **2010**, *6*, 3870.

45. Hough, L. A.; Islam, M. F.; Janmey, P. A.; Yodh, A. G. *Phys. Rev. Lett.* **2004**, *93*, 168102.

46. Ma, W. K.; Chinesta, F.; Ammar, A.; Mackley, M. R. *J. Rheol.* **2008**, *52*, 1311.